

# Genome-wide analysis of ascorbate-related oxidoreductases genes in *Actinidia arguta* provides new insights into ascorbic acid metabolic regulation during kiwifruit development

Xin Jiang<sup>1,2#</sup>, Chunli Yan<sup>2#</sup>, Xu Qiang<sup>2</sup>, Ting Ren<sup>1</sup>, Yanci Yang<sup>3</sup>, Ximing Chang<sup>1</sup>, Ying Zhang<sup>1\*</sup> and Yun Jia<sup>1\*</sup>

<sup>1</sup> Xi'an Botanical Garden of Shaanxi Province (Institute of Botany of Shaanxi Province), Xi'an, Shaanxi 710061, China

<sup>2</sup> Key Laboratory of Resource Biology and Biotechnology in Western China (Ministry of Education) College of Life Sciences, Northwest University, Xi'an, Shaanxi 710069, China

<sup>3</sup> School of Ecology and Environment, Baotou Teachers' College, Baotou, Inner Mongolia 014030, China

# Authors contributed equally: Xin Jiang, Chunli Yan

\* Correspondence: [zy@xab.ac.cn](mailto:zy@xab.ac.cn) (Zhang Y); [jiayun@xab.ac.cn](mailto:jiayun@xab.ac.cn) (Jia Y)

## Abstract

The ascorbate oxidase (AAO) and ascorbate peroxidase (APX) gene families are essential for the metabolic regulation of ascorbic acid. In this study, 25 AAO and 44 APX genes were identified in *A. arguta*, which were classified into three and five subfamilies, respectively. Syntenic analysis revealed that the expansion of these gene families was primarily driven by whole-genome duplication. Transcriptome analysis showed differential expression of AAO and APX genes across developmental stages in two kiwifruit cultivars. In addition, several key metabolites involved in the L-ascorbic acid pathway were detected, including L-ascorbic acid (AsA), dehydroascorbic acid, and oxidized glutathione. Notably, *AaAAO1*, *AaAAO5*, and *AaAPX3* showed correlations with AsA content. Furthermore, the expression patterns of six selected genes (*AaAPX2*, *AaAPX3*, *AaAPX4*, *AaAPX14*, *AaAAO15*, and *AaAAO16*) were further validated in two *A. arguta* varieties utilizing qRT-PCR. Overall, this study provides new insights into the identification and functional roles of AAO and APX gene families in *A. arguta* and highlights their role in regulating ascorbic acid metabolism.

**Citation:** Jiang X, Yan C, Qiang X, Ren T, Yang Y, et al. 2026. Genome-wide analysis of ascorbate-related oxidoreductases genes in *Actinidia arguta* provides new insights into ascorbic acid metabolic regulation during kiwifruit development. *Fruit Research* 6: e003 <https://doi.org/10.48130/frures-0025-0042>

## Introduction

Ascorbic acid (AsA), known as vitamin C, is a vital water-soluble antioxidant that plays essential roles in plant growth, development, and stress response, which functioned as a powerful scavenger of free radicals, activating the plant's antioxidant system to reduce the concentration of oxygen free radicals and mitigate the damage caused by reactive oxygen species (ROS)<sup>[1]</sup>. In addition to its antioxidant function, AsA is involved in various critical physiological processes<sup>[2]</sup>. For instance, it serves as an enzymatic cofactor in photosynthesis and acts as a photoprotectant to dissipate excess light energy<sup>[3]</sup>. AsA also contributes to cell division and expansion, osmotic adjustment, and hormone biosynthesis<sup>[4]</sup>. Moreover, it significantly enhances plant stress tolerance, such as improving salt tolerance by alleviating salt stress effects<sup>[5]</sup> and protecting against cold stress by neutralizing excess ROS<sup>[6]</sup>. Additionally, ascorbic acid regulates fruit ripening by efficiently eliminating ROS and modulating the cellular redox state, making it a key indicator of fruit nutritional value<sup>[7]</sup>. Understanding the mechanisms underlying vitamin C accumulation not only improves fruit quality but also facilitates the breeding of fruits with enhanced nutrition and agronomic traits<sup>[8]</sup>. Notably, ascorbate oxidase (AAO) and ascorbate peroxidase (APX) are essential antioxidant enzymes in plants, involved in the regeneration and degradation of ascorbic acid, thereby influencing its accumulation and, consequently, fruit ripening<sup>[9]</sup>. The major biosynthesis pathways of AsA currently recognized include the L-galactose pathway, L-gulose pathway, D-galacturonic acid pathway, and the inositol pathway<sup>[10]</sup>. APX exhibits the highest affinity among hydrogen peroxide-metabolizing enzymes<sup>[11]</sup>. It utilizes AsA as a specific electron donor to catalyze the reduction of hydrogen peroxide ( $H_2O_2$ ) to water and oxygen, while AsA itself is oxidized to

monodehydroascorbate (MDHA), thereby mitigating oxidative damage. APX plays a critical role during both fruit ripening and post-harvest, as it regulates  $H_2O_2$  and AsA levels, which directly affect fruit quality<sup>[9]</sup>. In contrast, AAO utilizes AsA as a substrate to generate ROS and also converts AsA to MDHA<sup>[4]</sup>. A decline in AsA content is temporally aligned with the onset of fruit ripening, indicated by color alterations, and is strongly associated with the upregulation of AAO activity<sup>[12]</sup>. This implies that AAO contributes critically to the ripening process by modulating AsA accumulation. Understanding the interaction between AAO and APX during fruit ripening offers valuable insights into the accumulation and stability of ascorbic acid.

In recent years, the APX gene family has been identified in various plants, with 11 in *Populus trichocarpa*<sup>[13]</sup> and eight in *Cannabis sativa*<sup>[14]</sup>. Based on subcellular localization, APX proteins are distributed in the cytoplasm, chloroplasts, peroxisomes, and mitochondria<sup>[15]</sup>. Increasing evidence suggests that APX proteins are pivotal for plant growth, development, and responses to abiotic stress<sup>[16]</sup>. Numerous studies have demonstrated that overexpression of APX genes enhances plant tolerance to abiotic stress, including heat, cold, drought, and salinity. For example, Wang et al. reported that overexpression of an APX gene family member from *Camellia azalea* increased heat and cold stress tolerance in tobacco plants<sup>[17]</sup>. Similarly, Liu et al. found that overexpression of *Apium graveolens* APX1 enhanced drought tolerance and increased ascorbic acid content in *Arabidopsis*<sup>[18]</sup>. Additionally, Zhang et al. demonstrated that loss of function in *OsAPX2* resulted in semi-dwarf seedlings, yellow-green leaves, leaf lesion mimics, and sterility in rice<sup>[19]</sup>. In contrast, studies on the AAO gene family remain limited, with existing research primarily focusing on *Gossypium hirsutum*<sup>[20]</sup>.

and *Beta vulgaris*<sup>[21]</sup>. However, AAO genes play multiple roles in plants, particularly in rapidly growing tissues and young fruits. Zhang et al. found that suppression of AAO expression resulted in increased ascorbic acid accumulation and improved fruit yield<sup>[22]</sup>, whereas upregulation of AAO expression led to reduced stomatal aperture in tobacco. Despite substantial progress in understanding the roles of APX and AAO in plants, their molecular mechanisms and specific functions in fruit development, ripening, and ascorbic acid accumulation remain unclear.

The kiwi berry (*Actinidia arguta*), a perennial vine of the Actinidiaceae family, is native to regions spanning from southwest China to the Russian Far East<sup>[23]</sup>. Often referred to as hardy kiwi, it differs from other kiwifruits by its typically sweeter flavor and the ability to be consumed whole without peeling. Additionally, *A. arguta* is rich in vitamin C and contains polyphenols, dietary fiber, and various other nutrients, which contribute to its potential in preventing chronic diseases and promoting human health<sup>[24]</sup>. Due to its favorable agricultural traits, including small fruit size and exceptional cold tolerance, along with its high nutritive value, *A. arguta* has gained increasing popularity among consumers<sup>[25]</sup>. Although significant progress has been made in various aspects of *A. arguta* research, such as its genetic characterization—exemplified by the recent genome assembly of *A. arguta*, which has paved the way for future functional genomics studies—there is still much to explore in terms of its bioactive ingredients<sup>[23]</sup>. For example, Leontowicz et al. compared the bioactivity and nutritional properties of *A. arguta* with those of *A. deliciosa* and *A. eriantha* and found that *A. arguta* exhibited superior bioactivity and nutritional value<sup>[26]</sup>. Antioxidants and nutrients, particularly ascorbic acid, have been among the most extensively studied compounds in *A. arguta*. However, most research has focused on comparisons with other *Actinidia* species and the dynamic changes in these compounds over time. It remains unclear how ascorbic acid accumulation is associated with the enzymes AAO and APX in *A. arguta*, particularly during its growth and development. While Lin et al. found significant correlations between AAO, APX, and AsA pool, the mechanisms underlying their interaction in regulating ascorbic acid accumulation and metabolism are still poorly understood<sup>[27]</sup>.

This study aims to identify all members of the APX and AAO gene families in *A. arguta* potentially involved in ascorbic acid regulation and to investigate their expression patterns and relationships to ascorbic acid accumulation during fruit development, with the goal of elucidating molecular mechanisms regulating ascorbic acid accumulation. To further validate the patterns of gene expression, two *A. arguta* cultivars with distinct fruit coloration were selected. 'Kukuba' (KKW), a Japanese cultivar, is characterized by its green flesh, elevated ascorbate content, and high antioxidant capacity, whereas 'Xiangziguang No. 1' (XZG), a Chinese cultivar, is distinguished by its red fruit pigmentation. These findings provide valuable insights into ascorbic acid regulation and may offer potential genetic resources for enhancing nutritional content and antioxidant capacity in *A. arguta*.

## Materials and methods

### Identification of gene members in *Actinidia* species

All APX and AAO protein sequences of *A. thaliana* were obtained from the TAIR database and used as query sequences. Candidate APX and AAO genes in *A. arguta* (*A. arguta* 'M', [Supplementary Table S1](#)) were identified by local BLASTP v2.15.0+ searches (E-value  $\leq 1e-5$ ) against the *A. arguta* genome. The resulting sequences were further examined with HMMER v3.3.2 and the PFAM database to confirm the presence of APX or AAO conserved domain<sup>[28,29]</sup>. Finally, sequences lacking the corresponding conserved structural domains were manually excluded from further analysis. Additionally, APX and AAO homologs from four *Actinidia* species (*A. chinensis* cv. Hongyang, *A. eriantha*, *A. hemisleyana*, and *A. rufa*) were consistently identified using the same approach as in *A. arguta* and retrieved from their respective genome databases ([Supplementary Table S1](#)). The isoelectric point (pI), molecular weight (MW), and instability indices of the identified AaAPX and AaAAO proteins were calculated by the ExPASy-ProtParam tool<sup>[30]</sup>. Subcellular localization of AaAPXs and AaAAOs was predicted using CELLO v.2.5<sup>[31]</sup>.

**Phylogenetic analysis**

Protein sequences of APX and AAO from *A. thaliana* and five *Actinidia* species were aligned using MUSCLE<sup>[32]</sup>. Phylogenetic trees were constructed with the neighbor-joining method in MEGA v7.0<sup>[33]</sup>, and classification of *A. arguta* family members was guided by previously reported clades in *Arabidopsis*. The resulting trees were visualized using the ggtree package in R v4.4.3<sup>[34]</sup>.

### Gene structure, conserved motifs, and cis-acting element analysis

Structural information of AaAPXs and AaAAOs was extracted from the *A. arguta* 'M' genome annotation (GFF files). Gene exon-intron structure was visualized utilizing the Gene Structure Display Server (<http://gsds.cbi.pku.edu.cn>). Protein sequences were aligned with ClustalW, and the alignments were displayed using TBtools v2.084<sup>[35,36]</sup>. Conserved motifs were identified through the MEME Suite<sup>[37]</sup>. For cis-regulatory analysis, 2.0 kb upstream promoter sequences of each AaAPX and AaAAO gene were retrieved from the genome and scanned for cis-acting elements using PlantCARE<sup>[38]</sup>. The identified elements were curated, formatted as BED files, and subsequently visualized with GSDS 2.0.

### Collinearity and selective pressure analysis

Syntenic relationships among gene family members were examined using MCScanX implemented in TBtools v2.084 with default settings<sup>[35,39]</sup>. Protein sequences were aligned in ParaAT v2.0 with MUSCLE<sup>[40]</sup>, and nonsynonymous (Ka) and synonymous (Ks) substitution rates were estimated using KaKs\_Calculator v2.0<sup>[41]</sup>. Selection pressure was inferred based on the Ka/Ks ratio, with values  $< 1$  indicating purifying selection and  $> 1$  indicating positive selection.

### Differential expression analysis of *A. arguta* APX and AAO gene family

To investigate the molecular mechanisms underlying antioxidant activity during kiwifruit development, previously generated transcriptomic and metabolomic datasets from the flesh of two *A. arguta* cultivars, Kukuba (KKW, full-green flesh) and Xianziguang No. 1 (XZG, red) (unpublished data from our laboratory), were analyzed. Fruit samples were collected from three replicate lianas at early fruit (T1, May 15<sup>th</sup>, approximately 20 d after full bloom), fruit ripening (T2, June 19<sup>th</sup>), and fully ripe (T3, September 15<sup>th</sup>) stages to represent the progression from early to full maturity, in the kiwifruit germplasm resource nursery at the Institute of Botany of Shaanxi province, Xi'an, China. A total of 18 samples (three biological replicates per developmental stage) were analyzed, with transcriptomic data

generated using the Illumina sequencing platform and metabolomic profiles obtained through comprehensive metabolite analysis by Metware Biotechnology Co, Ltd. (Wuhan, China). In the present study, these datasets were primarily examined to assess the expression of selected genes and the accumulation patterns of corresponding metabolites.

To explore the expression dynamics of *AaAPX* and *AaAAO* genes across the developmental stages of two *A. arguta* cultivars, clean reads were mapped to the *A. arguta* 'M' reference genome with HISAT2 v2.2.1<sup>[42]</sup>. Subsequently, transcript abundance was quantified with HTSeq and normalized as FPKM<sup>[43]</sup>. Differential expression between stages was assessed in DESeq2, applying  $|\log_2 \text{FC}| > 1$  &  $q$  value  $< 0.05$  as cutoffs<sup>[44]</sup>. Visualization of expression profiles was carried out by generating heatmaps in TBtools v2.084<sup>[35]</sup>. Finally, functional enrichment of the differentially expressed genes was examined through Gene Ontology (GO) analysis in the R package clusterProfiler v4.0<sup>[45]</sup>, with results plotted in ggplot2 under R v4.4.3<sup>[46]</sup>.

### Validation of key expressed genes by qRT-PCR

To examine the expression patterns of key genes (*AaAPX2*, *AaAPX3*, *AaAPX4*, *AaAPX14*, *AaAAO15*, and *AaAAO16*) in relation to key metabolites across two *A. arguta* varieties by qRT-PCR, total RNA was extracted utilizing TRIzol reagent (Invitrogen, Carlsbad, CA, USA), and then reverse-transcribed into complementary DNA (cDNA) using the FastQuant First Strand cDNA Synthesis Kit (Tiangen, Beijing, China). Primers for the target genes were designed utilizing Primer3Plus ([www.primer3plus.com](http://www.primer3plus.com)) (Supplementary Table S2). *Actinidia*  $\beta$ -actin was chosen as the reference gene for normalization<sup>[47]</sup>. The relative gene expression levels were determined by the  $2^{-\Delta\Delta C_t}$  method.

## Results

### Identification and characterization of the AAO and APX gene families in kiwifruit

In the present study, bioinformatics tools were employed to perform a genome-wide analysis of AAO and APX genes present in five *Actinidia* species and *A. thaliana*, as shown in Supplementary Table S3. A total of 14 to 44 AAOs and six to 25 APXs were identified in *Actinidia* plants, respectively (Supplementary Table S3). In the *A. arguta* 'M' genome, 25 *AaAAOs* (*AaAAO1*-*AaAAO25*) and 44 *AaAPXs* (*AaAPX1*-*AaAPX44*) genes were identified based on their order in chromosomes of the A and D sub-genomes, and dispersed across five and nine distinct chromosomes, respectively. Notably, the majority of these chromosomes contained only a single *AaAAO* or *AaAPX* gene. In contrast, two to three *AaAPX* genes were concurrently localized on chromosomes 21A-D and 11A-D, whereas two *AaAAO* genes were found on chromosomes 28A-D and 15A-B. Moreover, specific subsets of *AaAAO* (e.g., *AaAAO11*-*14*) and *AaAPX* (e.g., *AaAPX25*-*28*) genes exhibited co-localization on chromosomes 13, 23, and 28 within the A and D sub-genomes (Fig. 1).

The physicochemical properties analysis showed that the *AaAAO* proteins are composed of 475–799 amino acids and their molecular weights ranged from 53,245.32–88,873.57 Da, with isoelectric points of 5.7–6.96 for eight acidic proteins and 7.35–9.07 for 17 alkaline proteins. Similarly, the *AaAPX* proteins comprised 158–453 amino acids with molecular weights ranging from 18,078.65–48,956.51 Da, and isoelectric points ranging from 5.49–6.95 for 21 acidic proteins and from 7.57–9.6 for 23 alkaline proteins (Supplementary Tables S4, S5).

### Phylogenetic analysis

To investigate the evolutionary relationships of AAO and APX proteins among *Actinidia* plants, two separate phylogenetic trees were constructed: one for 69 AAOs and the other for 116 APXs from *A. thaliana*, *A. arguta*, *A. chinensis* 'Hongyang', *A. eriantha*, *A. hemisleyana*, and *A. rufa*. The model plant *A. thaliana* contains three putative AO genes, namely *At4g39830*, *At5g21105*, and *At5g21100*<sup>[48]</sup>. Further, classification results of the AAOs fell into three subfamily (Class I–III), encompassing 28, 12, and 29 proteins, respectively, and each labeled with a different colour (Fig. 2a). The APXs were divided into five subfamily (Class I–V), containing 34, 26, 14, 10, and 30 proteins, respectively (Fig. 2b). According to *A. thaliana* APXs<sup>[49]</sup>, clade I and II comprise cytosolic APXs, and clade III, V, IV mainly include chloroplastic APXs, as predicted by subcellular localization. The phylogenetic results obtained in this study are consistent with those reported previously<sup>[50]</sup>.

### Gene structure and conserved motifs analysis

The phylogenetic trees of all 25 *AaAAOs* (protein sequences) and 44 *AaAPXs* (protein sequences) in *A. arguta* were conducted separately, and their topological structures were consistent with those shown in Fig. 2. MEME was utilized to conduct further analysis of conserved motifs type and arrangement in *AaAAO* and *AaAPX* genes, and the results revealed that motifs ranged from six to ten in all AAO genes, with over half of the genes possessing ten conserved motifs, small half contained eight conserved motifs, among which motifs (1, 2, 3, 5, 7, 10) were the most conserved. In terms of the motifs in APX, nine conserved motifs were identified within these genes, and most of them demonstrated high similarity; however, several genes exhibited varying degrees of deletion. For instance, *AaAPX5* only contained motif 1 and motif 10, and *AaAPX22* encompassed motif 2, motif 3, motif 7, and motif 9. Besides, three conserved domains, PF07732, PF00394, and PF07731, were identified in all AAO gene family, PF00141 was identified in all APX gene family, indicating the accuracy of these genes (Fig. 3). A comparative analysis of exon–intron architectures was performed to characterize the evolutionary differences between the AAO and APX gene families in *A. arguta*. The structural characterization revealed that AAO genes generally exhibited simpler organizations, with most members containing only a single exon. In contrast, APX genes displayed significantly greater structural complexity, with exon numbers ranging from three to eight across different members. The sole exception was *AaAPX15*, which contained only two exons (Fig. 3).

### Analysis of cis-acting elements

A comprehensive *cis*-acting element analysis was performed on the promoter regions of AAOs and APXs in *A. arguta* to explore their potential regulatory roles. The identified *cis*-elements were primarily classified into four functional categories: hormone-responsive, light-responsive, stress-responsive, and growth and development-related elements. In addition, several elements were associated with flavonoid biosynthesis, metabolic regulation, and MYB binding, indicating potential regulatory roles of these genes in stress adaptation and secondary metabolism (Fig. 4). Interestingly, the number of *cis*-acting elements identified in APXs was higher than that in AAOs, implying that APXs may have a broader regulatory role in plant development and abiotic stress adaptation. Furthermore, ABRE elements—related to abscisic acid (ABA) responsiveness—were found in all *AaAAO* genes, except *AaAAO10* and *AaAAO20*, highlighting their potential involvement in hormone signaling pathways.

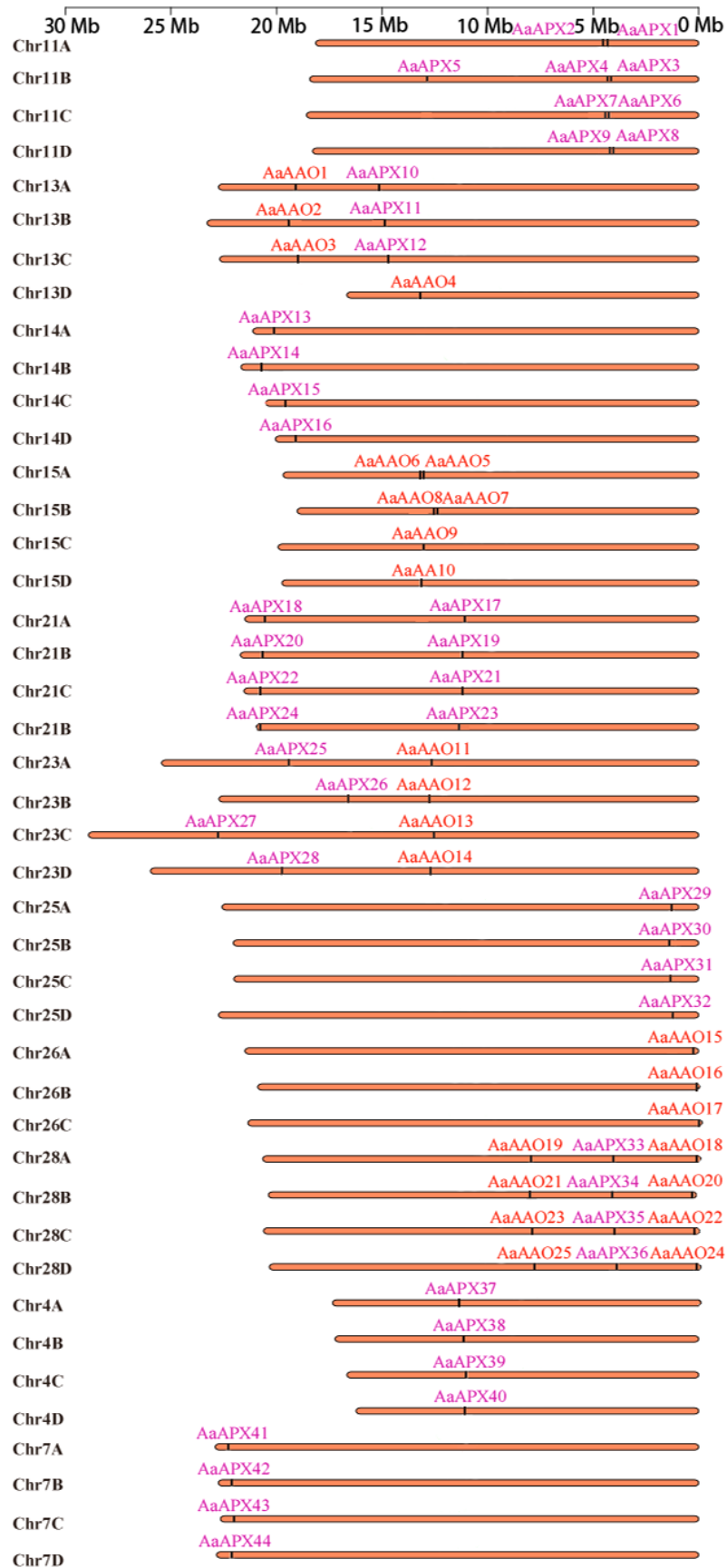


**Fig. 1** Distribution of *AaAO* and *AaAPX* genes on chromosome of *A. arguta*.

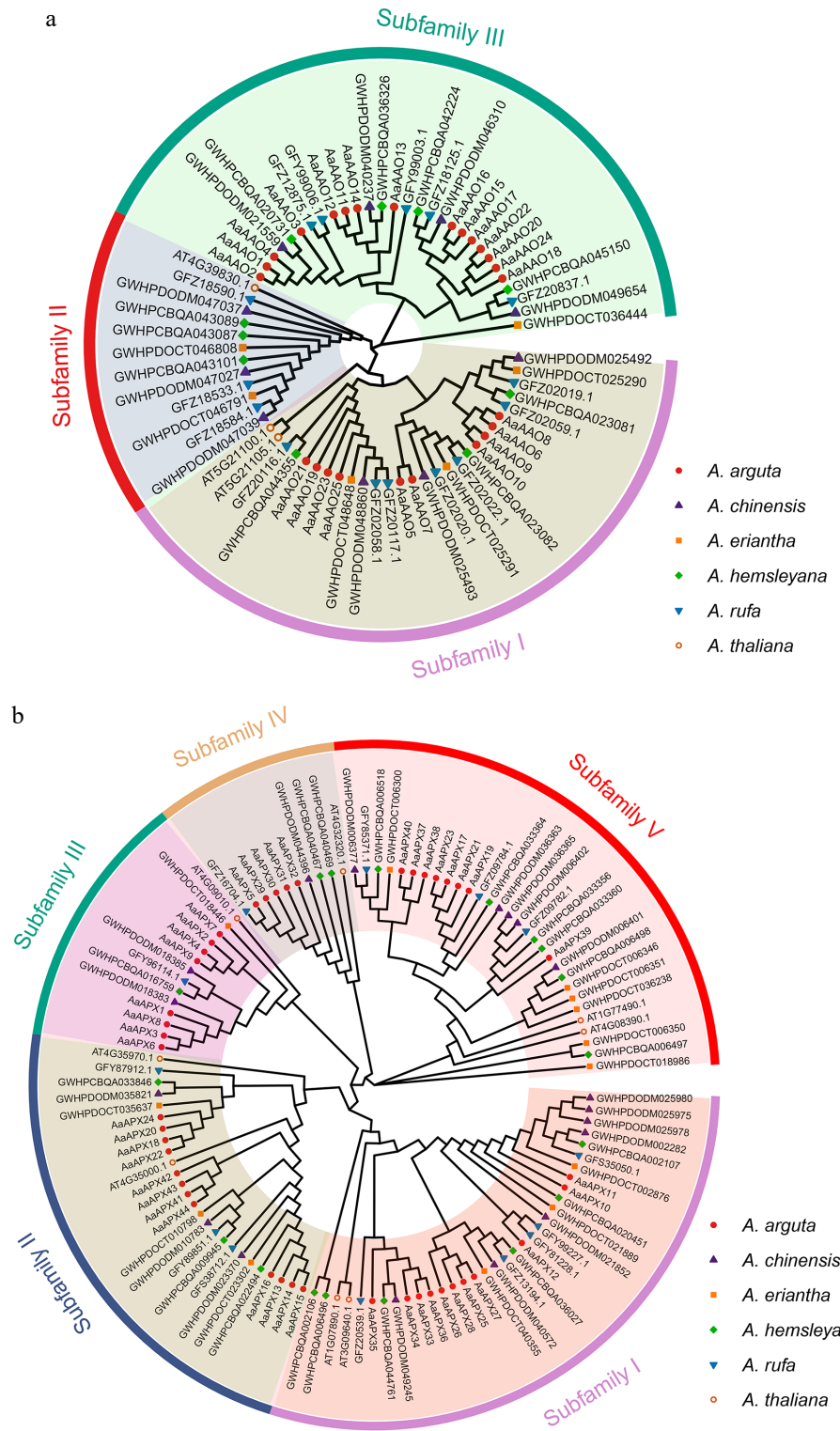


**Fig. 2** Phylogenetic analyses of the (a) AAO, and (b) APX families from five *Actinidia* species and *Arabidopsis*. Colored outer rings represent diverse subfamilies.

Meanwhile, Box 4 elements, indicative of light responsiveness, were present in all *AaAPX* genes, except *AaAPX7* and *AaAPX9*. These findings emphasize the likely participation of AAO and APX genes in hormonal regulation, light signaling, and stress-responsive networks during *A. arguta* fruit development (Fig. 4).

### Collinearity and selective pressure analysis

To clarify the expansion history of the AAO and APX gene families in *A. arguta*, duplication mode analysis was conducted. Most members were traced back to whole-genome (WGD) or segmental duplication events, suggesting that large-scale genome duplications were the primary driving force in their expansion. Additionally, two

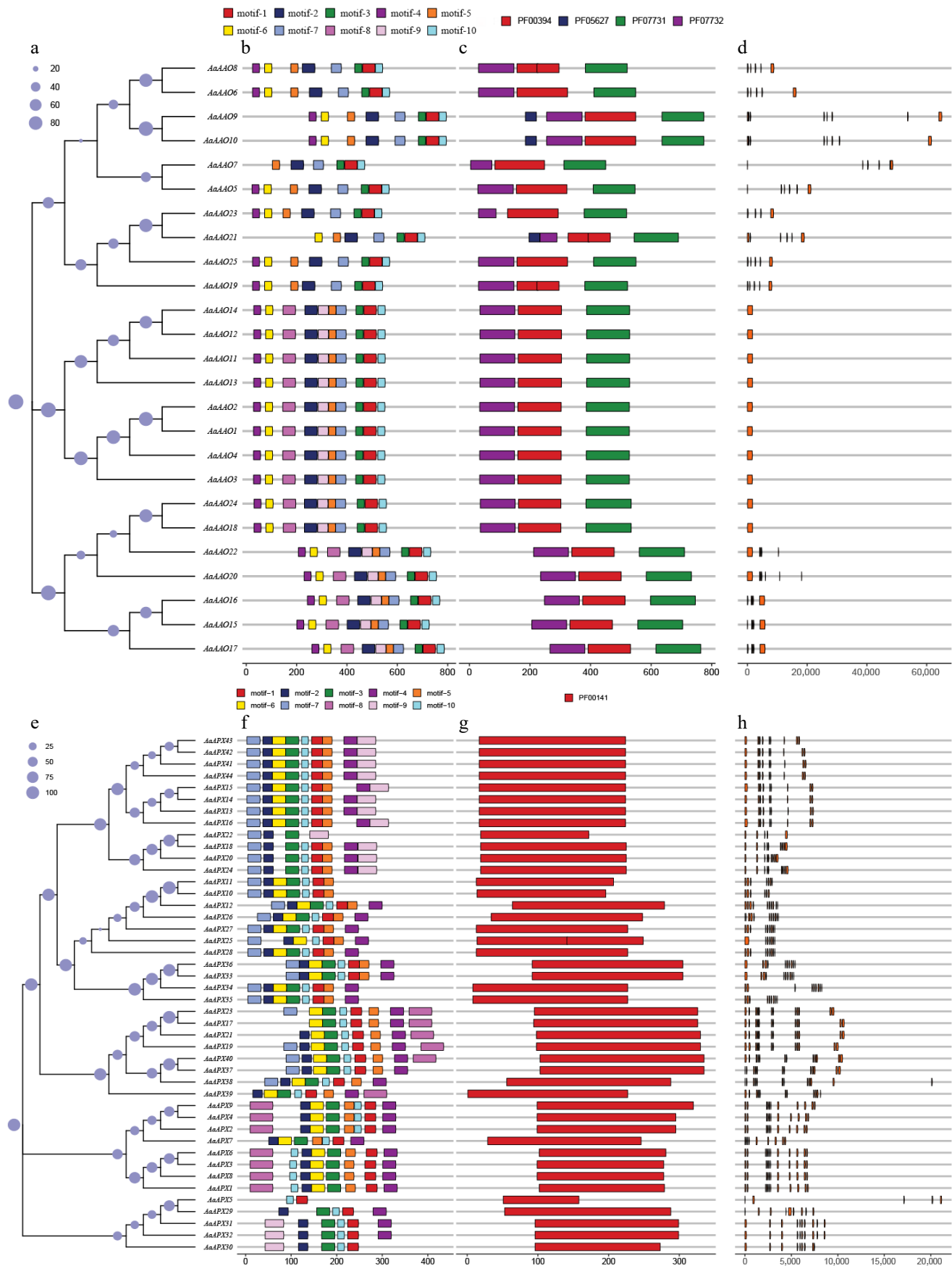


**Fig. 3** (a)–(d) shows the analysis of *AaAAOs* genes, and (e)–(h) shows the analysis of *AaAPXs* genes. (a), (e) Neighbor-joining trees constructed for *AaAAOs* and *AaAPXs* genes, respectively. (b), (f) Protein motifs, with motifs 1–10 displayed in different colored boxes. (c), (g) Conserved domains, represented by different colored boxes. (d), (h) Gene structures, where orange boxes represent CDS.

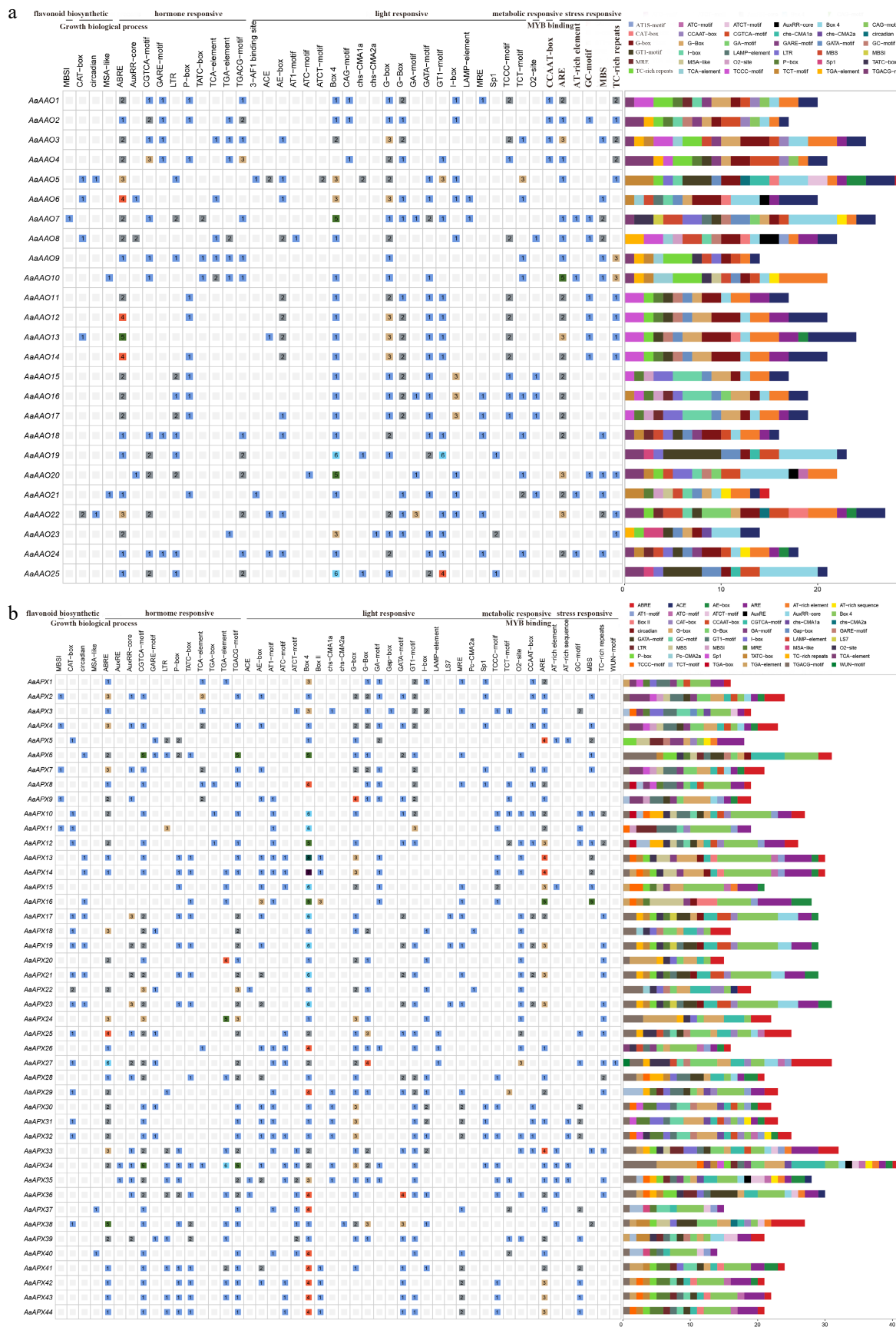


**Fig. 4** Predicted *cis*-elements within the 2,000 bp upstream region of *AaAO* and *AaAPX* genes. Different colors indicate distinct *cis*-element categories, with numbers displayed in the corresponding boxes. (a) *AO* gene family. (b) *APX* gene family.

AAO genes (*AaAAO6* and *AaAAO8*) exhibited tandem duplication (TD), while four APX genes (*AaAPX2*, *AaAPX4*, *AaAPX7*, and *AaAPX9*) experienced proximal duplication (PD) (Supplementary Table S6), further supporting the contribution of both large-scale and local duplication events to gene family expansion in *A. arguta* (Supplementary Table S6). Ka (non-synonymous substitution rate) and Ks (synonymous substitution rate) values were also calculated for homologous gene pairs within *A. arguta*, and the results showed that most of the Ka/Ks ratios were  $< 1$ , indicating that these gene pairs have undergone purifying selection during evolution in *A. arguta* (Supplementary Table S7).

To further explore the origins and evolutionary history of the AAO and APX gene families in *A. arguta* and the other three species, including *A. chinensis*, *A. eriantha*, and *A. thaliana*, a comparative synteny analysis was conducted. The analysis identified 18, 22, and three orthologous genomic APX gene pairs between *A. thaliana* and *A. arguta*, *A. chinensis* and *A. arguta*, *A. eriantha* and *A. arguta*, respectively. In contrast, there were no AAOs synteny results found between *A. arguta* and *A. eriantha*. A much higher degree of synteny was observed between *A. chinensis* and *A. arguta*, particularly on chromosome 28, which contained more orthologous gene pairs. Furthermore, the comparative analysis revealed that the number of APX genes was consistently lower than that of AAO genes across all four species, suggesting a differential expansion pattern between the two gene families (Fig. 5).

## Prediction of signal peptides

SignalP 6.0 was used to predict signal peptides in the AaAAO and AaAPX to evaluate their potential roles in secretion pathways. The AaAAO proteins exhibited a high likelihood of containing N-terminal signal peptides, with most genes showing signal peptide probabilities (SP(Sec/SPI)scores) exceeding 0.999, and predicted cleavage sites between amino acid positions 21 and 27. These findings suggest that AaAAO proteins are likely secreted, potentially playing a role in extracellular antioxidant activity. In contrast, the majority of

AaAPX proteins lacked predicted signal peptides, exhibiting signal peptide probabilities near zero, indicating their retention within the cytosol. However, *AaAPX26* was an exception, with an SP probability of 0.999589 and a predicted cleavage site at positions 21–22, suggesting a potential extracellular function for this protein (Supplementary Table S8). These results imply that AaAAO proteins may be involved in extracellular antioxidant defense, whereas AaAPX proteins primarily function within the cell, indicating their distinct subcellular roles in oxidative stress responses.

## Differential expression pattern of AAO and APX gene family

To investigate the potential role of the AAO and APX gene families in regulating L-ascorbate metabolism, expression patterns of these genes were analyzed in two *A. arguta* varieties (KKW and XZG) across three developmental stages. For example, *AaAPX14*, *AaAPX21*, and *AaAPX23* were predominantly downregulated in KKW at T1 but exhibited variable expression in other stages. In contrast, *AaAPX1*, *AaAPX6*, *AaAPX8*, and *AaAPX9* showed high expression levels in XZG at T1 in the Vitamin C biosynthesis (Fig. 6a, b). Notably, some antioxidant genes displayed consistent expression trends across different stages. For instance, *AaAPX38*, *AaAPX10*, and *AaAPX44* were significantly upregulated, whereas *AaAAO9*, *AaAPX39*, and *AaAPX34* were specifically downregulated at the T1, T2, and T3 stages, respectively. Interestingly, several genes exhibited significantly different expression patterns between the two varieties. For instance, *AaAAO1* and *AaAAO13* showed high expression levels at the first developmental stage in KKW, whereas *AaAAO19*, *AaAAO25*, and *AaAAO23* were highly expressed at the same stage in XZG (Fig. 6a, c). Pearson correlation coefficient analysis indicated that their expression levels were highly correlated (Pearson's  $r > 0.85$ ,  $p < 0.05$ ), such as *AaAAO10/AaAA23*, *AaAPX1/AaAPX6*, and *AaAAO8/AaAPX25* (Supplementary Fig. S1). However, the expression patterns of AaAAO and AaAPX genes varied between the two *A. arguta* varieties during the kiwifruit developmental stage (Supplementary Figs S2, S3).

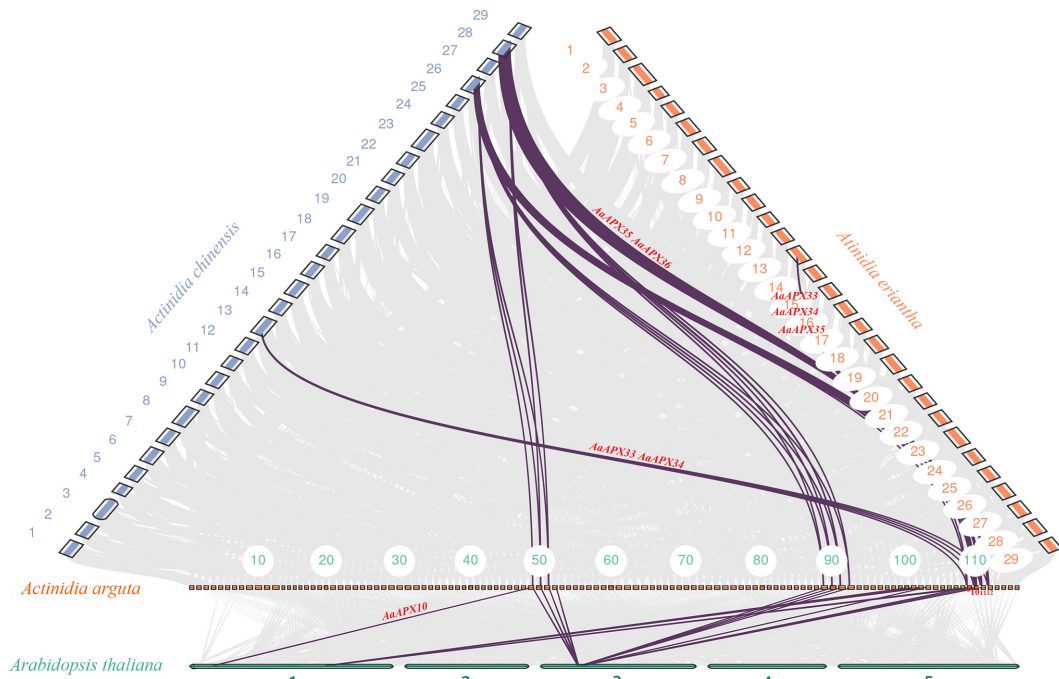


**Fig. 5** Collinearity analysis of the APX gene family between *A. arguta* and three related species (*A. thaliana*, *A. chinensis*, and *A. eriantha*). Gray lines indicate overall collinear regions, while colored lines denote orthologous gene pairs.

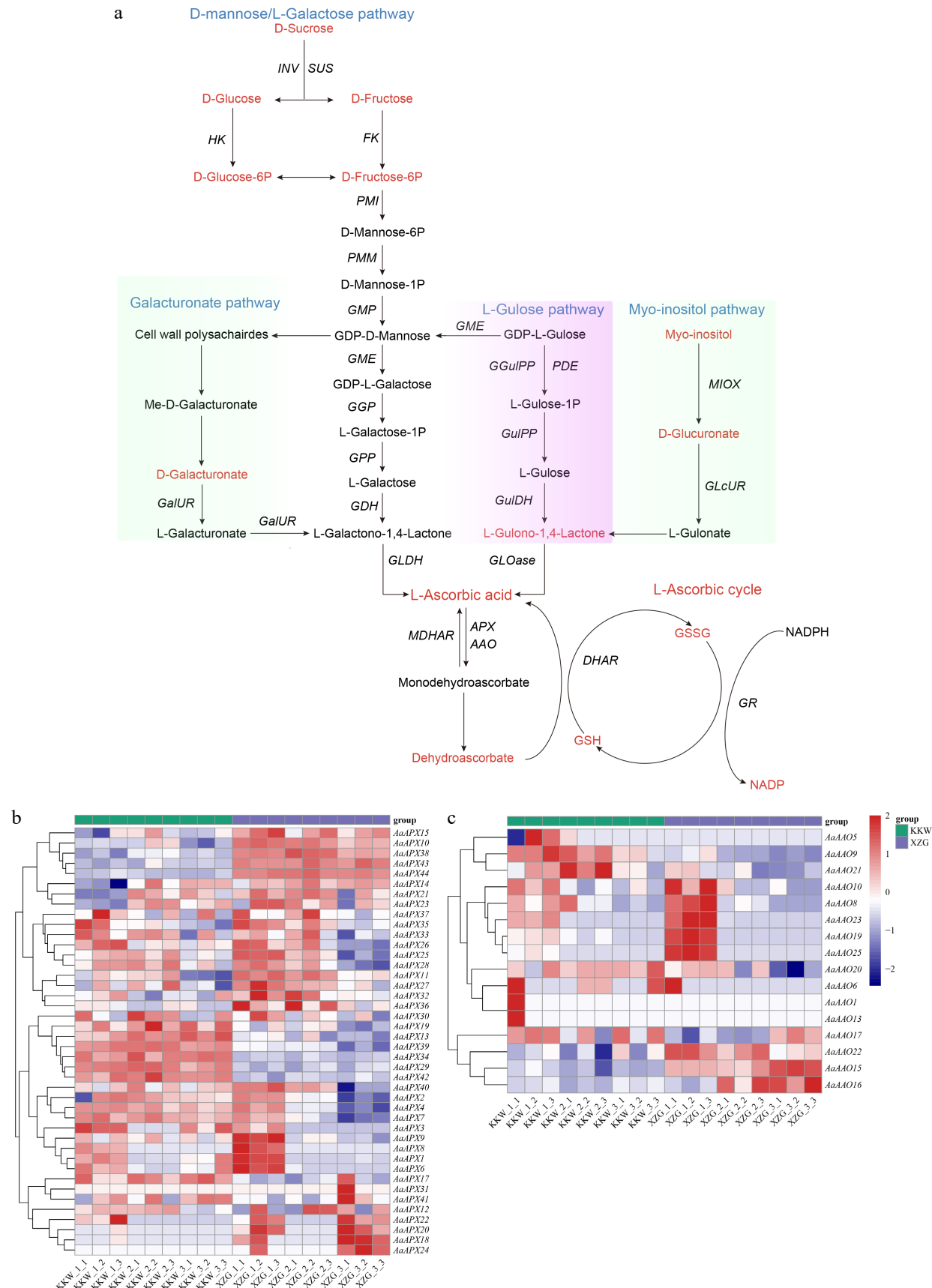


**Fig. 6** (a) Overview of the AsA metabolome profiles in two kiwifruit varieties. (b) Differential expression of *AaAPX* gene family members. (c) Differential expression of *AaAAO* gene family members.

Specifically, in comparisons between XZG and KKW, 16, 11, and nine genes were significantly upregulated, while six, 15, and ten genes were significantly downregulated at the T1, T2, and T3 stages, respectively (Supplementary Fig. S3). Furthermore, the distribution of transcription factor (TF) families between different developmental stages of KKW and XZG was explored, and the results revealed that the *bHLH* and *AP2/ERF* families show a high frequency of gene involvement. In contrast, other TF families like *WRKY*, *MYB*, and *NAC* display more moderate and consistent involvement across the stages, suggesting their stable regulatory roles throughout development (Supplementary Fig. S4).

To verify the accuracy of screened genes, six DEGs (*AaAPX2*, *AaAPX3*, *AaAPX4*, *AaAPX14*, *AaAAO15*, and *AaAAO16*) were selected for qRT-PCR analysis (Figs. 7, 8). The relative expression levels of *AaAPX3*, *AaAPX4*, *AaAPX14*, *AaAAO15*, and *AaAAO16* were higher in KKW than in XZG, indicating that these genes may be involved in cultivar-specific regulation. These results suggest that ascorbate-related oxidoreductases genes play complex regulatory and diverse roles in kiwifruit. Furthermore, the potential roles of APX and AAO gene family members were investigated; all identified gene members were subject to GO enrichment analyses. Except for partial gene members, such as *AaAAO16\_25*, that can't be annotated with corresponding functions, most of them were predominantly classified into four categories: L-ascorbate peroxidase activity, response to ROS, cellular response to oxidative stress, and hydrogen peroxide catabolic process (Supplementary Fig. S5).

### Correlation analysis of ascorbate-related genes during kiwifruit ripening

To investigate whether the expression levels of *AaAAO* and *AaAPX* genes are associated with L-ascorbate metabolism in kiwifruit, Pearson correlation coefficients (PCCs) were calculated between 69

genes and 13 related metabolites, including L-ascorbic acid, dehydroascorbic acid, and D-galacturonic acid, based on the four major AsA biosynthesis and recycling pathways (Fig. 8, Supplementary Table S9). The analysis revealed that *AaAAO1*, *AaAAO5*, *AaAAO13*, and *AaAPX3* were positively correlated with L-ascorbic acid levels, whereas *AaAPX14* showed a negative correlation with L-ascorbic acid.

Notably, it was observed that L-ascorbate displayed the highest accumulation at the developmental stage in KKW and then gradually declined during subsequent kiwifruit ripening, with a higher content than the other varieties at the T1 stage (Fig. 9). In contrast, XZG samples exhibited higher levels of fructose and glucose compared to KKW. Correlation analysis showed that *AaAAO15* and *AaAAO16* were positively correlated with fructose content, whereas *AaAAO6*, *AaAAO20*, *AaAPX2*, *AaAPX4*, and *AaAPX7* were negatively correlated with fructose (Fig. 8). Our analysis revealed strong connectivity between the *AaAAO* and *AaAPX* genes and related metabolites, highlighting their potential role in regulating L-ascorbate metabolism during kiwifruit ripening.

### Discussion

Ascorbic acid is essential for multiple physiological functions, especially in plant development, and serves as a powerful antioxidant that alleviates ROS accumulation<sup>[1]</sup>. Nevertheless, the functional interaction between AAO and APX in ascorbic acid homeostasis, and their influence on its fluctuation and fruit quality, remains poorly understood. While the genome-wide identification of APX genes has been extensively documented in various plant species, research on AAO has been relatively limited, with only a few studies reported in *G. hirsutum* and *B. vulgaris*<sup>[20,21]</sup>. Genome-wide identification in *A. arguta* uncovered 44 APX genes and 25 AAO genes. The

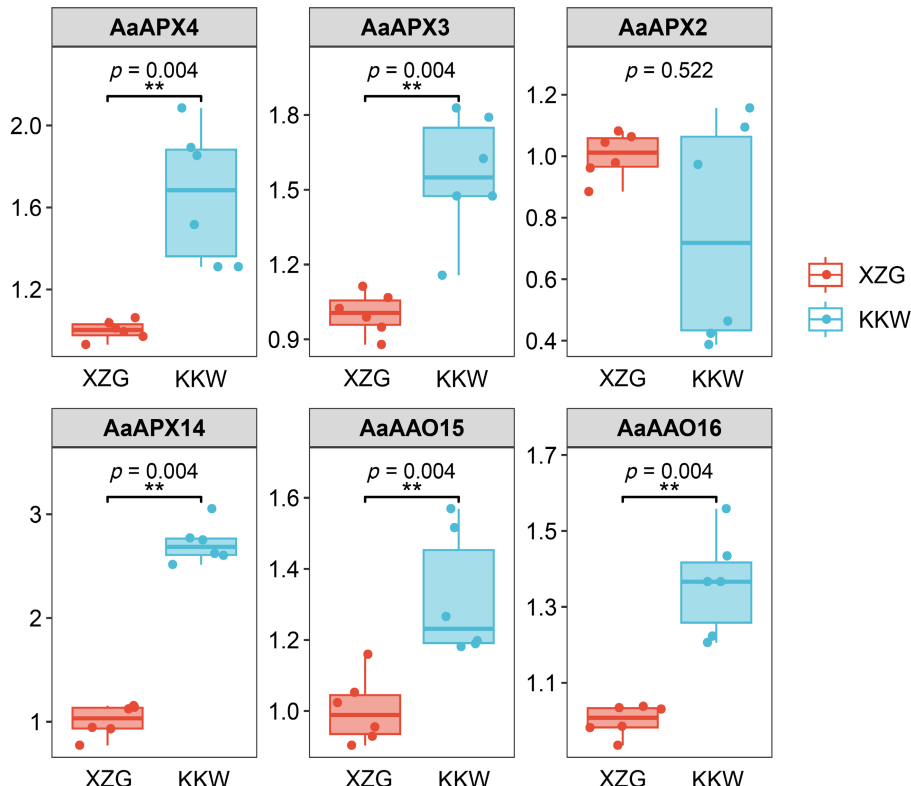


**Fig. 7** Results of qPCR analysis of the six selected *AaAPXs* in KKW and XZG.

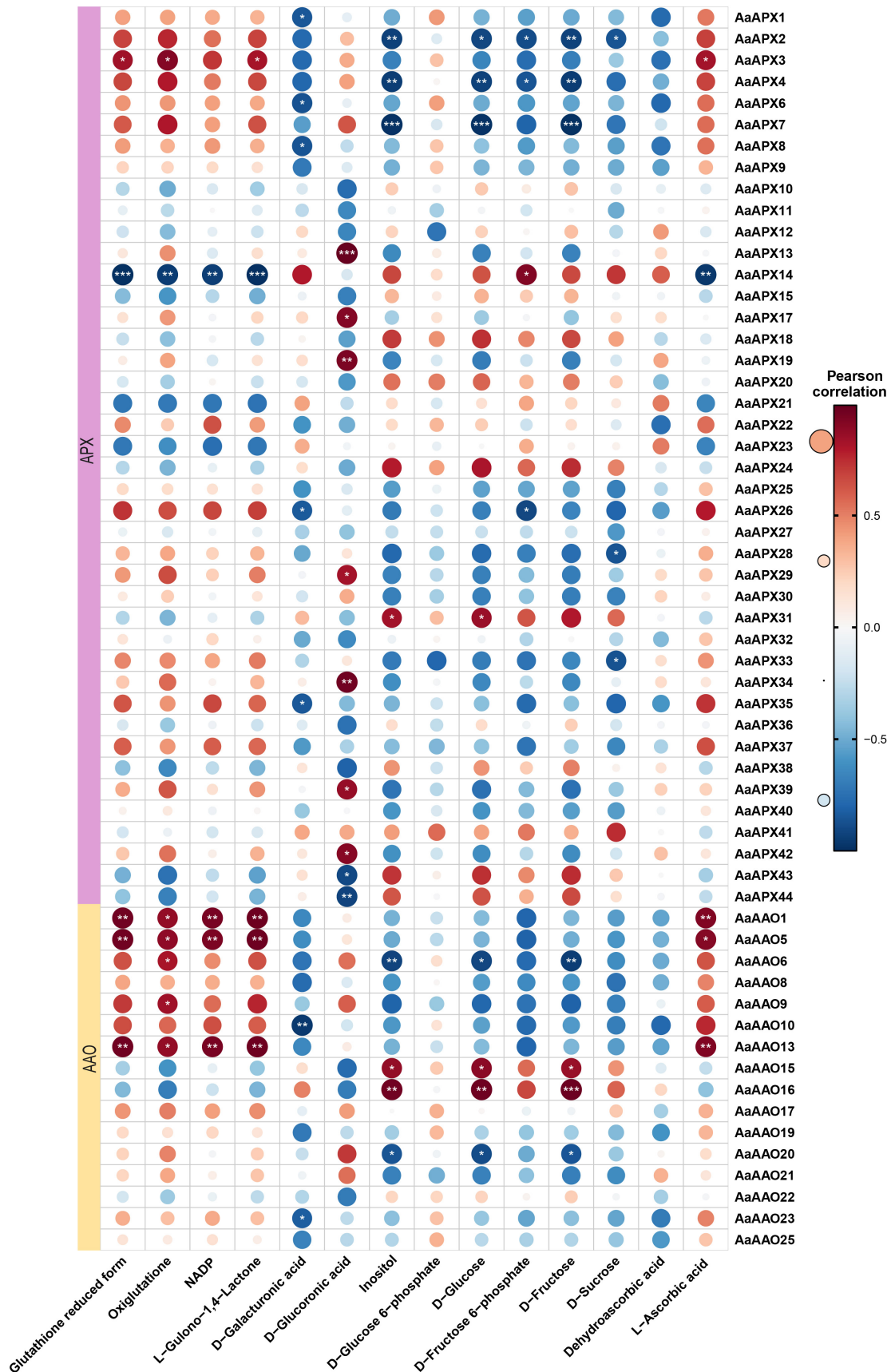


**Fig. 8** Correlation analysis between the expression of *AaAAO* and *AaAPX* genes and ascorbic acid-related metabolites in *A. arguta*. Red and blue color notes positive and negative correlations with gene expression, respectively.

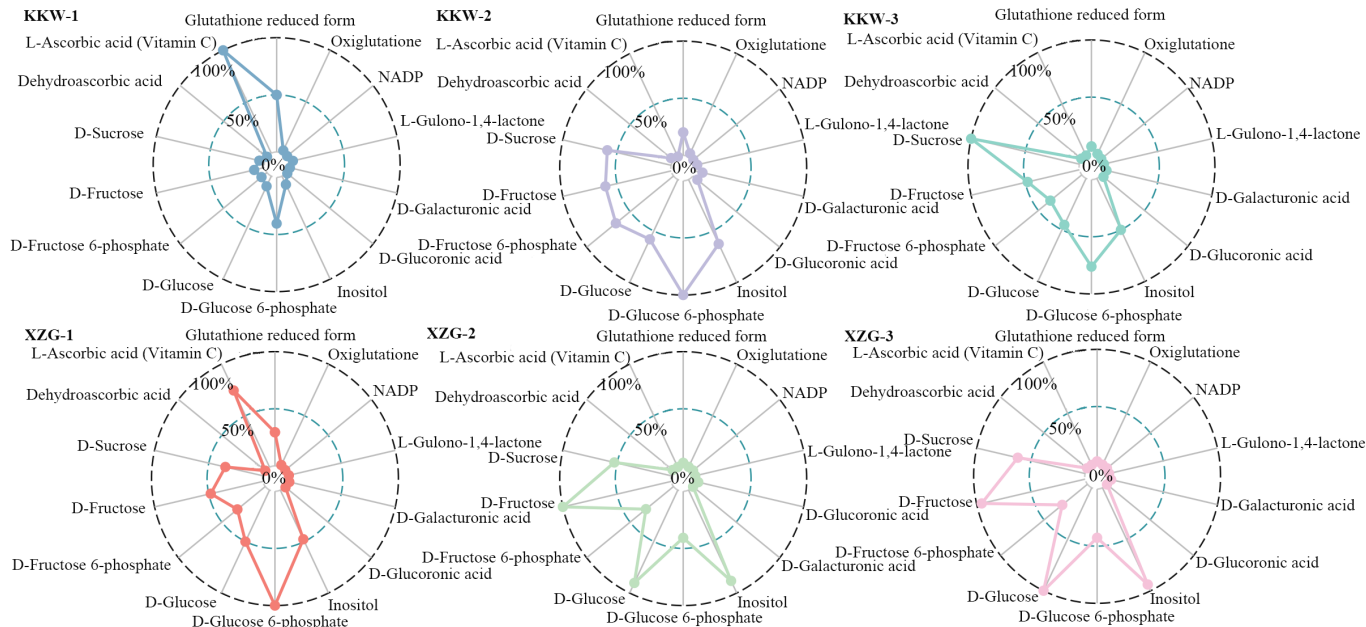


**Fig. 9** Comparison of the 13 representative metabolites between two kiwifruit varieties.

isoelectric points (pI) of APX and AAO ranged from 5.49–9.71 and 5.7–9.07, respectively, consistent with previous findings in other species<sup>[20,21]</sup>. For instance, the pI range of *CsAPX* was reported to be 5.54–8.87<sup>[14]</sup>, while that of *GhAO* was 5.65–8.63<sup>[20]</sup>. Subcellular localization analysis revealed that APX proteins were predominantly localized in the chloroplast (19/44) and cytoplasm (24/44), with only *AaAPX7* detected in the nucleus. In contrast, AAO proteins were mainly distributed in the vacuole (10/25), nucleus (7/25), and chloroplast (6/25), suggesting their potential functional roles in distinct organelles<sup>[51]</sup>. Furthermore, an uneven genomic distribution of AAO and APX gene family members was observed. For example, nine *AaAPX* genes were identified on chromosome 11, while no *AaAPX* genes were detected on chromosome 15. Similarly, *AaAAO* genes exhibited a clustered distribution, with eight genes located on chromosome 28 and none on chromosome 25. This uneven distribution may mirror the genetic variation and evolutionary trajectory of *A. arguta*, possibly driven by specific gene duplication events<sup>[52]</sup>.

Phylogenetic analysis provides key insights into gene family evolution, enabling the identification of orthologs, functional inference, and the detection of lineage-specific variations<sup>[53]</sup>. For instance, Liao et al. demonstrated that APX genes in *A. chinensis* could be classified into four phylogenetic groups, with genes sharing similar intron numbers clustering together<sup>[1]</sup>. Similarly, Pang et al. reported that nine *CaAPX* genes from pepper were grouped into five clades alongside APX genes from *A. thaliana*, rice, tomato, and potato<sup>[16]</sup>. In this study, 44 APX genes in the *A. arguta* genome were identified, which were classified into five distinct subfamilies similar to the previous study. Notably, genes such as *AaAPX1\_4*, *AaAPX6*, and *AaAPX8\_9*, localized to the chloroplast, clustered within the same subfamily, while others, including *AaAPX12*, *AaAPX17*, and *AaAPX19*, were grouped into different subfamilies. Additionally, 25 AAO genes were identified, which were also classified into three groups. Intriguingly, all vacuole-localized AAO proteins (e.g., *AaAAO1\_4* and *AaAAO11\_14*) clustered within subfamily III, alongside other members with distinct subcellular localizations. This phylogenetic pattern suggests a possible link between protein subfamily classification and localization, though experimental validation is required to confirm this hypothesis<sup>[53]</sup>.

Gene duplication events, including tandem repeats and segmental duplications, are critical mechanisms for expanding gene families by generating homologous genes and increasing gene copy numbers<sup>[54]</sup>. In this study, 44 *AaAPX* and 25 *AaAAO* genes were identified, most of which originated from whole-genome duplication (WGD) events, highlighting the significant role of WGD in the expansion of *AaAPX* and *AaAAO* gene families in *A. arguta*. Furthermore, the Ka/Ks analysis revealed that the majority of homologous gene pairs exhibited Ka/Ks ratios < 1 (Supplementary Table S7), indicating that *AaAPX* and *AaAAO* genes have undergone purifying selection during their evolutionary history. *Cis*-acting elements are critical regulators of plant gene expression and play an indispensable role in mediating plant responses to environmental changes and evolutionary adaptations<sup>[55]</sup>. It's widely reported that members of the APX gene family are involved in abiotic stress responses. For instance, Li et al. reported that the loss of any APX genes in *A. thaliana* led to reduced stress tolerance during both germination and maturation stages, underscoring the functional importance of these genes in stress adaptation<sup>[56]</sup>. In this study, Box 4, ARE, and ABRE were identified as the predominant *cis*-regulatory elements in the promoters of APX genes, with 142, 75, and 68 occurrences, respectively. These elements are primarily associated with light response, stress response, and hormone signaling (Fig. 4), highlighting the pivotal role of APX genes in regulating key physiological processes in plants<sup>[57]</sup>. As a species characteristically thriving in and well-adapted to sun-exposed environments, the high abundance of light-responsive *cis*-regulatory elements in its APX genes may reflect an evolutionary adaptation to optimize light utilization and enhance stress tolerance. Interestingly, it was also observed that ABRE (50 occurrences), Box 4 (47 occurrences), and ARE (43 occurrences) were the dominant *cis*-regulatory elements in the promoters of AAO genes. The predominance of ABRE elements, which are associated with hormone signaling, suggests that APX and AAO genes may share overlapping functional roles in mediating plant responses to hormonal and environmental stimuli. Notably, the light-responsive ATCT motif and Gap box were uniquely predicted in *AaAAO5* and *AaAPX3*, respectively. The unique presence of these regulatory elements may be associated with their putative functions as key

regulators. These findings provide valuable insights into the regulatory mechanisms underlying the stress-responsive and hormone-mediated functions of APX and AAO gene families in *A. arguta*. Further investigation into the specific roles of these *cis*-regulatory elements could enhance our understanding of their contributions to plant development, adaptation, and evolution<sup>[58]</sup>.

Extensive studies have documented the variation in APX gene expression among different tissues in multiple plant species. For instance, Pang et al. investigated the expression profiles of *CaAPX* genes in different tissues of pepper and found that *CaAPX8* exhibited consistently high expression levels across all tissues except at the F-Dev5 stage<sup>[16]</sup>. Similarly, Aleem et al. utilized RNA-seq data to analyze the expression patterns of APX genes in fourteen soybean tissues, revealing that the majority of APX genes displayed tissue-specific expression patterns, highlighting their functional diversity<sup>[59]</sup>. Here, expression patterns of APX and AAO genes were examined across three developmental stages in *A. arguta*, and AsA content was detected in the three stages to explore the relationship between the accumulating level and the degradation/regeneration of AsA. In fact, the AsA content across the three developmental stages represents a net outcome of the balance between its *de novo* biosynthesis, degradation, and regeneration. In a previous study, *AcAO1* and *AcAPX2* were identified as key genes in the AsA recycling pathway. At 10 DPA, despite high expression levels of biosynthetic genes, the AsA content was low—a phenomenon that coincided with the peak expression of both *AcAO1* and *AcAPX2* and the highest accumulation of L-dehydroascorbate. Functional genomic validation subsequently confirmed that the AsA pool at this stage is primarily regulated by the recycling pathway<sup>[60]</sup>. In Stage I, the observed peak in AsA accumulation is driven by active biosynthesis to support rapid cell division and morphogenesis. Critically, this stage was characterized by the most robust transcriptional activity, as the majority of genes within both the APX and AAO gene families exhibited their highest expression levels, with the greatest number of highly expressed genes occurring in Stage I compared to the subsequent stages (Fig. 6b, c). The concurrent high expression of APX and AAO genes in Stage I reflects a dynamic balance in AsA metabolism. APX-driven regeneration maintains the reduced AsA pool, whereas AAO-mediated degradation likely serves to actively fine-tune the pool size and redox signaling for proper development. Specifically, *AaAAO1*, *AaAAO13*, *AaAAO19*, and *AaAAO25*, exhibited significantly higher expression levels at the first developmental stage in both KKW and XZG cultivars compared to the other two stages (Fig. 6c). In contrast, during Stages II and III, the significant decrease in AsA content correlates with a predicted decline in biosynthetic activity. This period was marked by a widespread downregulation in both AAO and APX gene expression, indicating a coordinated reduction in the entire metabolic flux of AsA encompassing both its regenerative turnover and its degradative consumption. This collective downregulation reflects a metabolic shift away from the high demand of active growth towards a lower maintenance requirement in maturing tissues. However, Specific APX genes, such as *AaAPX18*, *AaAPX24*, and *AaAPX31*, displayed the highest expression levels during the third developmental stage. As supported by Liu et al., the initial low accumulation at 10 DPA can be attributed to intense degradation and regeneration, evidenced by the high expression of APXs and AAOs, particularly AAOs<sup>[60]</sup>. The subsequent peak around 20 DPA was primarily driven by active biosynthesis, coupled with a relative decline in APX and AAO expression (though their levels remained substantial). Finally, the decrease in AsA during ripening was mainly caused by reduced biosynthesis, with degradation/regeneration processes also contributing.

GO enrichment analysis indicated that these genes are mainly associated with responses to ROS (Supplementary Fig. S5), implying a potential role in ROS scavenging and oxidative stress regulation during fruit development. Correlation analysis revealed strong co-expression between *AaAPX18* and *AaAPX24* (Supplementary Fig. S1), suggesting a coordinated role in antioxidant metabolism. Phylogenetic analysis further indicates that both genes cluster with the *A. thaliana* APX gene *At4g35000* (Fig. 2b), which is known to participate in ROS detoxification and redox homeostasis<sup>[16]</sup>. This homology implies that *AaAPX18* and *AaAPX24* may serve conserved roles in regulating oxidative balance during fruit development, meriting further functional validation. Moreover, the positive correlations of *AaAAO1*, *AaAAO5*, and *AaAPX3* with L-ascorbic acid suggest their involvement in ascorbate accumulation, whereas the negative correlation of *AaAPX14* may indicate a role in ascorbate turnover. While this study documented dynamic changes in AsA content and identified key candidate genes in the two varieties, the molecular mechanisms responsible for the varietal differences are not yet fully understood. Elucidating the precise roles of these genes, including their specific contributions to the regeneration and degradation processes that govern AsA dynamics, will require further molecular validation through techniques such as functional genomics. Collectively, these findings shed light on the temporal regulation of APX and AAO gene expression and their roles in stress responses and developmental processes in *A. arguta*. Further functional studies are needed to clarify their contributions to redox homeostasis, stress tolerance, and ascorbic acid biosynthesis in kiwifruit.

## Conclusions

In this study, a comprehensive genome-wide analysis of APX and AAO genes in *A. arguta* was performed, identifying 44 APX and 25 AAO members. Phylogenetic analysis revealed that both APX and AAO genes could be classified into five and three distinct groups. A potential correlation between protein subfamily classification and subcellular localization was observed, although further experimental validation is required to confirm this hypothesis. Additionally, APX and AAO gene family members were unevenly distributed across different chromosomes, a pattern likely attributable to gene duplication events during evolution. Expression analysis of APX and AAO genes across three developmental stages revealed that AAO and APX genes exhibited relatively higher expression levels in the first stage in both KKW and XZG cultivars. Notably, *AaAPX18* and *AaAPX24* displayed the highest expression levels during the third developmental stage, suggesting a potential synergistic effect in mediating ROS scavenging and mitigating oxidative damage. The AsA level peaked at 20 DPA, driven predominantly by active biosynthesis, and subsequently declined during ripening mainly due to attenuated biosynthesis. Consistently, the expression of AAO and APX genes, which was relatively strong in the initial phase, also weakened alongside the biosynthetic process. This finding highlights their critical role in maintaining cellular homeostasis during late developmental stages. These results provide comprehensive insights into the genomic organization, evolutionary dynamics, and functional roles of APX and AAO gene families in *A. arguta*. Further investigation into the regulatory mechanisms and synergistic interactions of these genes could enhance our understanding of their contributions to antioxidant defense, ascorbate accumulation, and biosynthesis.

## Author contributions

The authors confirm contribution to the paper as follows: study conception and design: Jia Y; data collection: Qiang X; analysis and interpretation of results: Jia Y, Qiang X, Jiang X, Yan C; technical assistance: Qiang X, Ren T, Yang Y, Chang X, Zhang Y; draft manuscript preparation: Jia Y, Jiang X, Yan C. All authors reviewed the results and approved the final version of the manuscript.

## Data availability

All data generated or analyzed during this study are included in this published article and supplementary information files.

## Acknowledgments

This research was supported by the National Natural Science Foundation of China (Grant No. 32300314), the Shaanxi Academy of Science Research Funding Project (Grant Nos 2022K-09, 2024p-12), and the Xi'an Botanical Garden of Shaanxi Province Young Talent Funding Project (Grant No. 2024TJ-02).

## Conflict of interest

The authors declare that they have no conflict of interest.

**Supplementary information** accompanies this paper online at (<https://doi.org/10.48130/frures-0025-0042>)

## Dates

Received 18 July 2025; Revised 3 November 2025; Accepted 25 November 2025; Published online 21 January 2026

## References

- [1] Liao GL, Liu Q, Li YQ, Zhong M, Huang CH, et al. 2020. Identification and expression profiling analysis of ascorbate peroxidase gene family in *Actinidia chinensis* (Hongyang). *Journal of Plant Research* 133(5):715–726
- [2] Chaturvedi S, Khan S, Bhunia RK, Kaur K, Tiwari S. 2022. Metabolic engineering in food crops to enhance ascorbic acid production: crop biofortification perspectives for human health. *Physiology and Molecular Biology of Plants* 28(4):871–884
- [3] Maruta T. 2022. How does light facilitate vitamin C biosynthesis in leaves? *Bioscience, Biotechnology, and Biochemistry* 86(9):1173–1182
- [4] Smirnoff N. 2018. Ascorbic acid metabolism and functions: a comparison of plants and mammals. *Free Radical Biology & Medicine* 122:116–129
- [5] Kakan X, Yu Y, Li S, Li X, Huang R, et al. 2021. Ascorbic acid modulation by ABI4 transcriptional repression of VTC2 in the salt tolerance of *Arabidopsis*. *BMC Plant Biology* 21(1):112
- [6] Liu X, Bulley SM, Varkonyi-Gasic E, Zhong C, Li D. 2023. Kiwifruit bZIP transcription factor AcePosF21 elicits ascorbic acid biosynthesis during cold stress. *Plant Physiology* 192(2):982–999
- [7] Arabia A, Munné-Bosch S, Muñoz P. 2024. Ascorbic acid as a master redox regulator of fruit ripening. *Postharvest Biology and Technology* 207:112614
- [8] Fenech M, Amaya I, Valpuesta V, Botella MA. 2019. Vitamin C Content in Fruits: Biosynthesis and Regulation. *Frontiers in Plant Science* 9:2006
- [9] Liao G, Chen L, He Y, Li X, Lv Z, et al. 2021. Three metabolic pathways are responsible for the accumulation and maintenance of high AsA content in kiwifruit (*Actinidia eriantha*). *BMC Genomics* 22(1):13
- [10] Valpuesta V, Botella MA. 2004. Biosynthesis of L-ascorbic acid in plants: new pathways for an old antioxidant. *Trends in Plant Science* 9(12):573–577
- [11] Li HB, Qin YM, Pang Y, Song WQ, Mei WQ, et al. 2007. A cotton ascorbate peroxidase is involved in hydrogen peroxide homeostasis during fibre cell development. *The New Phytologist* 175(3):462–471
- [12] Yahia EM, Contreras-Padilla M, Gonzalez-Aguilar G. 2001. Ascorbic acid content in relation to ascorbic acid oxidase activity and polyamine content in tomato and bell pepper fruits during development, maturation and senescence. *LWT - Food Science and Technology* 34(7):452–457
- [13] Leng X, Wang H, Zhang S, Qu C, Yang C, et al. 2021. Identification and characterization of the APX gene family and its expression pattern under phytohormone treatment and abiotic stress in *Populus trichocarpa*. *Genes* 12(3):334
- [14] Liang Z, Xu H, Qi H, Fei Y, Cui J. 2024. Genome-wide identification and analysis of ascorbate peroxidase (APX) gene family in hemp (*Cannabis sativa* L.) under various abiotic stresses. *PeerJ* 12:e17249
- [15] Shen L, Zhou Y, Yang X. 2024. Genome-wide identification of ascorbate peroxidase (APX) gene family and the function of *SmAPX2* under high temperature stress in eggplant. *Scientia Horticulturae* 326:112744
- [16] Pang X, Chen J, Xu Y, Liu J, Zhong Y, et al. 2023. Genome-wide characterization of ascorbate peroxidase gene family in pepper (*Capsicum annuum* L.) in response to multiple abiotic stresses. *Frontiers in Plant Science* 14:1189020
- [17] Wang J, Wu B, Yin H, Fan Z, Li X, et al. 2017. Overexpression of *CaAPX* induces orchestrated reactive oxygen scavenging and enhances cold and heat tolerances in tobacco. *BioMed Research International* 2017(1):4049534
- [18] Liu J, Hasanuzzaman M, Wen H, Zhang J, Peng T, et al. 2019. High temperature and drought stress cause abscisic acid and reactive oxygen species accumulation and suppress seed germination growth in rice. *Protoplasma* 256(5):1217–1227
- [19] Zhang Z, Zhang Q, Wu J, Zheng X, Zheng S, et al. 2013. Gene knockout study reveals that cytosolic ascorbate peroxidase 2(OsAPX2) plays a critical role in growth and reproduction in rice under drought, salt and cold stresses. *PLoS One* 8(2):e57472
- [20] Pan Z, Chen L, Wang F, Song W, Cao A, et al. 2019. Genome-wide identification and expression analysis of the ascorbate oxidase gene family in *Gossypium hirsutum* reveals the critical role of *GhAO1A* in delaying dark-induced leaf senescence. *International Journal of Molecular Sciences* 20(24):6167
- [21] Skorupa M, Szczepanek J, Yolcu S, Mazur J, Tretyn A, et al. 2022. Characteristic of the ascorbate oxidase gene family in *Beta vulgaris* and analysis of the role of AAO in response to salinity and drought in beet. *International Journal of Molecular Sciences* 23(21):12773
- [22] Zhang Y, Li H, Shu W, Zhang C, Zhang W, et al. 2011. Suppressed expression of ascorbate oxidase gene promotes ascorbic acid accumulation in tomato fruit. *Plant Molecular Biology Reporter* 29(3):638–645
- [23] Lu XM, Yu XF, Li GQ, Qu MH, Wang H, et al. 2024. Genome assembly of autotetraploid *Actinidia arguta* highlights adaptive evolution and enables dissection of important economic traits. *Plant Communications* 5(6):100856
- [24] Pinto D, Delerue-Matos C, Rodrigues F. 2020. Bioactivity, phytochemical profile and pro-healthy properties of *Actinidia arguta*: a review. *Food Research International* 136:109449
- [25] Hu YK, Kim SJ, Jang CS, Lim SD. 2024. Antioxidant activity analysis of native *Actinidia arguta* cultivars. *International Journal of Molecular Sciences* 25(3):1505
- [26] Leontowicz H, Leontowicz M, Latocha P, Jesion I, Park YS, et al. 2016. Bioactivity and nutritional properties of hardy kiwi fruit *Actinidia arguta* in comparison with *Actinidia deliciosa* 'Hayward' and *Actinidia eriantha* 'Bidan'. *Food Chemistry* 196:281–291
- [27] Lin Y, Zhao B, Tang H, Cheng L, Zhang Y, et al. 2022. L-ascorbic acid metabolism in two contrasting hardy kiwifruit (*Actinidia arguta*) cultivars during fruit development. *Scientia Horticulturae* 297:110940
- [28] Finn RD, Clements J, Eddy SR. 2011. HMMER web server: interactive sequence similarity searching. *Nucleic Acids Research* 39:W29–W37
- [29] Mistry J, Chuguransky S, Williams L, Qureshi M, Salazar Gustavo A, et al. 2020. Pfam: The protein families database in 2021. *Nucleic Acids Research* 49:D412–D419

[30] Gasteiger E, Hoogland C, Gattiker A, Duvaud Se, Wilkins MR, et al. 2005. Protein identification and analysis tools on the ExPASy server. In *The Proteomics Protocols Handbook*. Ed. Walker JM. Totowa, NJ: Humana Press. pp. 571–607 doi: [10.1385/1-59259-890-0:571](https://doi.org/10.1385/1-59259-890-0:571)

[31] Chou KC, Shen HB. 2010. Cell-PLoc 2.0: an improved package of web-servers for predicting subcellular localization of proteins in various organisms. *Natural Science* 2(10):1090–1103

[32] Edgar RC. 2004. MUSCLE: multiple sequence alignment with high accuracy and high throughput. *Nucleic Acids Research* 32(5):1792–1797

[33] Kumar S, Stecher G, Tamura K. 2016. MEGA7: molecular evolutionary genetics analysis version 7.0 for bigger datasets. *Molecular Biology and Evolution* 33(7):1870–1874

[34] Yu G. 2020. Using ggtree to visualize data on tree-like structures. *Current Protocols in Bioinformatics* 69(1):e96

[35] Chen C, Wu Y, Li J, Wang X, Zeng Z, et al. 2023. TBtools-II: a “one for all, all for one” bioinformatics platform for biological big-data mining. *Molecular Plant* 16(11):1733–1742

[36] Thompson JD, Gibson TJ, Plewniak F, Jeanmougin F, Higgins DG. 1997. The CLUSTAL\_X windows interface: flexible strategies for multiple sequence alignment aided by quality analysis tools. *Nucleic Acids Research* 25(24):4876–4882

[37] Bailey TL, Boden M, Buske FA, Frith M, Grant CE, et al. 2009. MEME SUITE: tools for motif discovery and searching. *Nucleic Acids Research* 37:W202–W208

[38] Lescot M, Déhais P, Thijs G, Marchal K, Moreau Y, et al. 2002. PlantCARE, a database of plant cis-acting regulatory elements and a portal to tools for in silico analysis of promoter sequences. *Nucleic Acids Research* 30(1):325–327

[39] Wang Y, Tang H, Debarry JD, Tan X, Li J, et al. 2012. MCScanX: a toolkit for detection and evolutionary analysis of gene synteny and collinearity. *Nucleic Acids Research* 40(7):e49

[40] Zhang Z, Xiao J, Wu J, Zhang H, Liu G, et al. 2012. ParaAT: a parallel tool for constructing multiple protein-coding DNA alignments. *Biochemical and Biophysical Research Communications* 419(4):779–781

[41] Wang D, Zhang Y, Zhang Z, Zhu J, Yu J. 2010. KaKs\_Calculator 2.0: a toolkit incorporating gamma-series methods and sliding window strategies. *Genomics, Proteomics & Bioinformatics* 8(1):77–80

[42] Kim D, Paggi JM, Park C, Bennett C, Salzberg SL. 2019. Graph-based genome alignment and genotyping with HISAT2 and HISAT-genotype. *Nature Biotechnology* 37(8):907–915

[43] Putri GH, Anders S, Pyl PT, Pimanda JE, Zanini F. 2022. Analysing high-throughput sequencing data in Python with HTSeq 2.0. *Bioinformatics* 38(10):2943–2945

[44] Love MI, Huber W, Anders S. 2014. Moderated estimation of fold change and dispersion for RNA-seq data with DESeq2. *Genome Biology* 15(12):550

[45] Wu T, Hu E, Xu S, Chen M, Guo P, et al. 2021. clusterProfiler 4.0: A universal enrichment tool for interpreting omics data. *Innovation* 2(3):100141

[46] Shannon P, Markiel A, Ozier O, Baliga NS, Wang JT, et al. 2003. Cytoscape: a software environment for integrated models of biomolecular interaction networks. *Genome Research* 13(11):2498–2504

[47] Ampomah-Dwamena C, McGhie T, Wibisono R, Montefiori M, Hellens RP, et al. 2009. The kiwifruit lycopene beta-cyclase plays a significant role in carotenoid accumulation in fruit. *Journal of Experimental Botany* 60(13):3765–3779

[48] Lim CK. 2012. *The function of ascorbate oxidase in Arabidopsis thaliana*. Doctoral thesis. University of Exeter, United Kingdom

[49] Panchuk II, Zentgraf U, Volkov RA. 2005. Expression of the Apx gene family during leaf senescence of *Arabidopsis thaliana*. *Planta* 222(5):926–932

[50] Guo K, Du X, Tu L, Tang W, Wang P, et al. 2016. Fibre elongation requires normal redox homeostasis modulated by cytosolic ascorbate peroxidase in cotton (*Gossypium hirsutum*). *Journal of Experimental Botany* 67(11):3289–3301

[51] Sami A, Haider MZ, Shafiq M, Sadiq S, Ahmad F. 2024. Genome-wide identification and in-silico expression analysis of CCO gene family in sunflower (*Helianthus annuus*) against abiotic stress. *Plant Molecular Biology* 114(2):34

[52] Bao P, Sun J, Qu G, Yan M, Cheng S, et al. 2024. Identification and expression analysis of CCCH gene family and screening of key low temperature stress response gene *CbuC3H24* and *CbuC3H58* in *Catalpa bungei*. *BMC Genomics* 25(1):779

[53] Gao R, Chen L, Chen F, Ma H. 2024. Genome-wide identification of SHMT family genes in alfalfa (*Medicago sativa*) and its functional analyses under various abiotic stresses. *BMC Genomics* 25(1):781

[54] Wang C, Xiong S, Hu S, Yang L, Huang Y, et al. 2024. Genome-wide identification of Gα family in grass carp (*Ctenopharyngodon idella*) and reproductive regulation functional characteristics of Cignaq. *BMC Genomics* 25(1):800

[55] Wang F, Sun F, Yu Z, Zhang Y, Liu Y, et al. 2025. Genome-wide identification of glyoxalase (*PbrGLY*) gene family and functional analysis of *PbrGLYI-28* in response to Botryosphaeria dothidea in pear. *BMC Plant Biology* 25(1):349

[56] Li ZQ, Li JT, Bing J, Zhang GF. 2019. The role analysis of APX gene family in the growth and developmental processes and in response to abiotic stresses in *Arabidopsis thaliana*. *Hereditas* 41(6):534–547

[57] Shafiq A, Chauhan R, Gill T, Swarnkar MK, Sreenivasulu Y, et al. 2015. Expression of SOD and APX genes positively regulates secondary cell wall biosynthesis and promotes plant growth and yield in *Arabidopsis* under salt stress. *Plant Molecular Biology* 87(6):615–631

[58] Marand AP, Eveland AL, Kaufmann K, Springer NM. 2023. cis-Regulatory elements in plant development, adaptation, and evolution. *Annual Review of Plant Biology* 74:111–137

[59] Aleem M, Aleem S, Sharif I, Aleem M, Shahzad R, et al. 2022. Whole-genome identification of APX and CAT gene families in cultivated and wild soybeans and their regulatory function in plant development and stress response. *Antioxidants* 11(8):1626

[60] Shu P, Zhang Z, Wu Y, Chen Y, Li K, et al. 2023. A comprehensive metabolic map reveals major quality regulations in red-flesh kiwifruit (*Actinidia chinensis*). *The New Phytologist* 238(5):2064–2079



Copyright: © 2026 by the author(s). Published by Maximum Academic Press, Fayetteville, GA. This article is an open access article distributed under Creative Commons Attribution License (CC BY 4.0), visit <https://creativecommons.org/licenses/by/4.0/>.